



HAL
open science

Kinetic analysis of the thermal degradation of an intumescent fire retardant coated green biocomposite

M. Rashid, K. Chetehouna, A. Settar, J. Rousseau, C. Roudaut, L. Lemée, Z. Aboura

► To cite this version:

M. Rashid, K. Chetehouna, A. Settar, J. Rousseau, C. Roudaut, et al.. Kinetic analysis of the thermal degradation of an intumescent fire retardant coated green biocomposite. *Thermochimica Acta*, 2022, 711, pp.179211. 10.1016/j.tca.2022.179211 . hal-04060290

HAL Id: hal-04060290

<https://hal.science/hal-04060290>

Submitted on 22 Jul 2024

HAL is a multi-disciplinary open access archive for the deposit and dissemination of scientific research documents, whether they are published or not. The documents may come from teaching and research institutions in France or abroad, or from public or private research centers.

L'archive ouverte pluridisciplinaire **HAL**, est destinée au dépôt et à la diffusion de documents scientifiques de niveau recherche, publiés ou non, émanant des établissements d'enseignement et de recherche français ou étrangers, des laboratoires publics ou privés.



Distributed under a Creative Commons Attribution - NonCommercial 4.0 International License

Kinetic analysis of the thermal degradation of an intumescent fire retardant coated green biocomposite

M. Rashid^{a,*}, K. Chetehouna^a, A. Settar^a, J. Rousseau^b, C. Roudaut^b, L. Lemée^b, Z. Aboura^c

a. INSA Centre Val de Loire, Univ. Orléans, PRWASME EA 4229, F-18022, Bourges, France

b. Université de Poitiers, CNRS UMR 7285 (IC2MP), 4 Rue M. Brunet, 86073, Poitiers Cedex 9, France

c. Laboratoire Roberval, Université de Technologie de Compiègne, UMR-CNRS 7337 Centre de Recherche de Royallieu, 60203 Compiègne, France

*Corresponding author: Madiha RASHID

INSA Centre Val de Loire, Univ. Orléans, PRWASME EA 4229, F-18022, Bourges, France

Email address: madiha.rashid@insa-cvl.fr

Abstract

This study focuses on the thermal degradation behaviour of a newly developed fire retardant coated green biocomposite (GBC) and its kinetic analyses under inert and oxidative atmosphere. An intumescent fire retarding system comprised of ammonium polyphosphate-tris (2-hydroxyethyl) isocyanurate (APP-THEIC) and boric acid is used to improve fire retardancy of GBC. Multiples formulations having different proportions of APP-THEIC and boric acid are developed to study the heat shielding effect and morphology of the material. The fire retardant coated GBC is characterised using Thermo Gravimetric Analysis (TGA) and Scanning Electron Microscopy (SEM). TGA showed similar thermal decomposition profile for fire retardant coated specimens except for E/20APP-THEIC/10BA showing reduced decomposition rate after 650°C and higher amount of residual char as compared to other coatings. However, SEM images revealed better morphology for E/29APP-THEIC/1BA, which indicates improved thermal insulation to the underlying substrate. The evaluation of the degradation of such materials are quite expensive at industrial scale since the heating rates are extremely high and it was not possible to evaluate the thermal decomposition behaviour of the intumescent fire retardant (IFR) coated GBC directly by TGA at very high heating rates. Therefore, it is imperative to develop predictive models for kinetics of degradation of such materials. In this research study, the controlled and IFR coated GBC has been thermally decomposed at three different heating rates and a predictive model for its kinetics of degradation has been determined. Kinetics Neo software package developed by Netzsch Company is used to establish a kinetic model for the decomposition of controlled and IFR coated green biocomposite. The decomposition mechanism and degradation products of the controlled (uncoated) and IFR coated GBC allowed for the interpretation of the kinetic decomposition models.

35 **Keywords:** TGA, Kinetic analysis, Intumescent coating, fitting model, SEM

36 **1. Introduction**

37 In recent years, bio-based composites were replacing traditional materials in different
38 industrial sectors, mainly construction and transport industries. This recent surge is motivated
39 by factors, such as depletion of fossil reserves, high cost petroleum, and the current shift
40 toward environmentally friendly and sustainable “green” composite materials supported by
41 the implementation of environmental legislation such as REACH Act (Registration,
42 Evaluation, Authorization and Restriction of Chemical substances) [1]–[4]. Despite numerous
43 benefits, such as increased fuel efficiency, light weight vehicles, sound mechanical properties,
44 low cost, less maintenance, low energy consumption in fabrication and end of life disposal
45 [5]–[7] the commercial use of green biocomposite is still unpopular in commercial domain.
46 This is due to some inherent disadvantages, such as weak adhesion between hydrophilic
47 natural fibre and hydrophobic biopolymers, poor moisture absorption, low thermal stability,
48 and poor fire resistance [8]. In past decades, bio-based materials have been mainly used as
49 flexible or rigid packaging materials where stringent flammability measures were not strictly
50 followed. The growing use of green biocomposites in the transportation and electronics
51 sector necessitate the use of strategies to improve flammability to meet the fire safety
52 standards of these sectors.

53 Fire retardancy is a phenomenon in which the ignitibility of the material is reduced or, if they
54 were ignitable, should burn with less efficiency [9]. Several strategies exist for fire retardancy
55 of green biocomposites, such as chemical modification, surface treatment, use of inherently
56 fire resistant polymers, and direct incorporation of Flame-Retardants (FRs) and/or micro or
57 nanoparticles in materials. Among these approaches “passive fireproofing of materials”, in
58 which Intumescent Fire Retardant (IFR) coating is applied on the material to decrease the heat
59 transfer to the structure being protected is a well-known technique. The use of fire retarded
60 coating is one of the oldest, easiest, and efficient way to protect a substrate against fire [10],
61 [11]. This technique offers several advantages, such as preserving the intrinsic properties of
62 the material (e.g. the mechanical properties), easy processing and its application on several
63 materials, such as polymers [12], metallic materials [13], and wood [14].

64 This protection mechanism is activated when the material is exposed to heat; the coating starts
65 to melt and converts into highly viscous liquid. Simultaneously, reactions were initiated that
66 result in the release of inert gases, and these gases were trapped inside the viscous fluid

67 (formation of bubbles). Consequently, the expansion or foaming of the coating takes place,
68 upto several times its original thickness, to form a protective carbonaceous char that plays the
69 role of insulating barrier between the fire and the substrate as shown in Figure 1 [15].



70
71

Figure 1: Degradation of an IFR coating

72 An ideal IFR coating allows a balance between fire retardant properties and the amount of
73 additives in the coating. Mostly, it is comprised of three intumescent ingredients i.e. an acid
74 source, a carbon source and a blowing agent. The ingredients of the formulation of these
75 coatings need to be adapted to form an efficient protective char. In the mechanism of
76 intumescence the acid source breaks down to yield a mineral acid, then the dehydration of the
77 carbonizing agent takes place to yield carbon char, and lastly the blowing agent decomposes
78 to form gaseous products [10], [16]–[18]. The blowing agent causes the char to swell and an
79 insulating multi-cellular protective layer is formed. This protective shield limits the transfer of
80 heat from the heat source to the material and the transfer of mass from the material to the heat
81 source resulting in a protection of the underlying material. To form an efficient intumescent
82 fire protection system, it is essential that the different components of the formulation exhibit a
83 synergistic behaviour. A random selection of components from each class mentioned above
84 does not ensure efficient intumescent behaviour. Therefore, it is necessary to study the
85 thermal degradation behaviour of IFR coating with different formulation to ascertain the
86 presence components that exhibit synergistic effect to produce efficient coating. In this
87 context, ammonium polyphosphate coated with tris (2-hydroxyethyl) isocyanurate
88 (commercially known as IFR36) and boric acid were employed to form an efficient IFR
89 system to protect green biocomposite against fire.

90 Ammonium polyphosphate (APP) is moderately water-insoluble high melting solid, that
91 contains high phosphorous content (up to 30%) . There were several crystalline forms of APP

92 having different molecular mass, solubility and particle size. Phosphorus is known to promote
93 char formation that forms a protective coating. Phosphoric acids resulting from phosphate
94 esters were used in coatings and protect the underlying substrate similar to borate glass that
95 were formed when borax and boric acid were used [19]. The IFR coating generally use
96 resinous binder as the base of mixture [9], [20], [21]. Boron compounds act as fire
97 suppressants in both vapour and condensed phase. Boron complexes were mostly Lewis acids,
98 which promote crosslinking of polymers on thermal degradation of the material that
99 consequently minimise decomposition of polymer and release of combustible volatile. They
100 react with a hydroxyl group in the polymeric material to form a glassy ester, which
101 procedures char on the surface of substrate and reduces solid-state oxidation by protecting the
102 underlying material [22]. Boric acid releases chemically bonded water to dilute the
103 concentration of pyrolytic fuel, inhibits the release of combustible gases from burning
104 cellulosic materials and dehydrates oxygen-containing polymers to form char that further
105 inhibits combustion [23], [24].

106 Thermo Gravimetric Analysis (TGA) is employed in this study to investigate the thermal
107 stability of the controlled specimens of GBC as well as the IFR coated GBC. The possible
108 interactions among the components of formulation and the reactivity of the system will also
109 be examined to identify the efficacy of the IFR formulation. Scanning electron microscopy is
110 used to examine the morphology and structure of the thermally degraded material. There exist
111 state of the art testing to evaluate the efficiency of fire protective coating, but these tests were
112 expensive which limits the research development of IFR coatings. Therefore, small-scale test
113 were carried out, such as TGA coupled with mathematical modelling were used in order to
114 predict the efficiency and the performance of the coatings [25]. The detailed mechanisms of
115 the degradation reactions of flame retarded polymers were generally complex [26], [27]
116 therefore in order to integrally model the thermal decomposition of a material, it is imperative
117 to use a model that takes into account different steps of the thermal decomposition. The
118 understanding of degradation mechanism of green biocomposites and the study of their
119 kinetics is particularly important since they have direct impact on processing conditions,
120 properties, and applications of these materials. Therefore, in order to further this study, it is
121 deemed essential to determine the key kinetic parameters that govern the thermal
122 decomposition of these materials. Kinetic studies of thermal decomposition provide essential
123 information on the mechanisms and thermal degradation behaviour through kinetic
124 parameters. These kinetic parameters can be determined by fitting various kinetic models that

125 explain thermal decomposition of material under specific conditions [28]. Once a kinetic
126 model is validated for particular set of reaction, numerical simulation tools could be used to
127 define the characteristics of properties, such as flame spread at higher critical conditions
128 where it becomes very difficult to perform full-scale fire experiments[29][30][31][32].

129 The objective of this research study is to analyse the thermal degradation of various samples
130 under inert and oxidative conditions using TGA, study kinetics of thermal degradation of IFR
131 coated GBC via model-fitting approach and perform morphological analysis of thermally
132 decomposed GBC using SEM and EDS.

133 **2. Material and Methods**

134 2.1. Materials

135 Natural fibre reinforcement of 2x2-twill weave flax fibre having an areal density of 550 g/m²
136 was procured from Eco-technilin, France. A 38% biobased thermoset epoxy, InfuGreen 810,
137 was purchased from Sicomin, France. A fire retardant system containing ammonium
138 polyphosphate $[\text{NH}_4 \text{PO}_3]_n(\text{OH})_2$ and tris (2-hydroxyethyl) isocyanurate (C₉H₁₅N₃O₆)
139 abbreviated as APP-THEIC and commercially known as Exolit IFR36 was used along with
140 boric acid (H₃BO₃) abbreviated as BA to form a fire retardant coating. Exolit IFR36 was a
141 product of Clariant, Germany and boric acid was bought from Sigma Aldrich, France.

142 2.2. Methodology for preparation of new biobased composite

143 The resin part of InfuGreen810 was mixed with SD 8822 curing agent in the ratio of 100:31
144 w:w. The prepared epoxy was infused, under vacuum pressure of -0.9 bar at room
145 temperature, using vacuum bag resin transfer moulding into the six stacked plies of flax fibre
146 that were placed on top of each other with a stacking sequence of [0]₆ to manufacture the
147 green biocomposite as shown in Figure 2. The infused plates were left to cure for a period of
148 24 hours at room temperature and then post cured for 16 hours at 60°C in an oven to complete
149 the polymerisation reaction. The manufacturing of green biocomposite has been demonstrated
150 in detail in a previous work by Rashid et al. [33].



Figure 2: Vacuum bag resin transfer moulding of flax reinforcement using Infugreen 810

151

152

153 The resin part of Infugreen 810 was used as a binder for the fire retarding agents, APP-
 154 THEIC and boric acid, that were present in the form of powder. Ammonium polyphosphate-
 155 THEIC and boric acid were mixed in the resin for about 20 minutes, using a mechanical
 156 mixer, at room temperature and pressure. SD 8822 (curing agent) was then added in the
 157 mixture of resin and fire retardants, and the formulation was stirred for 15 more minutes. The
 158 total quantity of flame retardant, in the IFR coating formulations, was always kept 30 wt.%.
 159 The amount of ammonium polyphosphate-THEIC and boric acid (BA) was varied between
 160 five different ratios as shown in Table 1 Table 1 to determine the most effective fire retardant
 161 formulation having balanced amount of additives that exhibit synergism for the protection of
 162 green biocomposite. In Table 1 , E was designated as abbreviation for infugreen810 epoxy
 163 and TH stands for THEIC. The quantity of fire retardants in the coating formulations was kept
 164 as following; C1: 20 wt.% APP-THEIC and 10 wt.% boric acid, C2: 25 wt.% APP-THEIC
 165 and 5 wt.% boric acid, C3: 27 wt.% APP-THEIC and 3 wt.% boric acid, C4: 29 wt.% APP-
 166 THEIC and 1 wt.% boric acid and C4: 30 wt.% APP-THEIC.

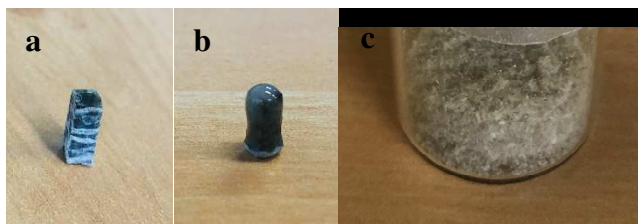
167 **Table 1:** Formulation of IFR coating

No.	Formulation	APP-TH wt. %	BA wt. %	Resin wt. %	Hardner wt. %
C1	E/20APP-TH/10BA	20	10	54	16
C2	E/25APP-TH/5BA	25	5	54	16
C3	E/27APP-TH/3BA	27	3	54	16
C4	E/29APP-TH/1BA	29	1	54	16
C5	E/30APP-TH	30	0	54	16

168

169 The prepared IFR coating was applied using a brush on the specimens cut to the dimension of
 170 2×2×6.5mm (Figure 3a and 3b), as shown in Figure 2b. The curing cycle of 24hours at room
 171 temperature and post curing of 16hours at 60°C in an oven was repeated to complete the
 172 polymerisation reaction. The thickness of applied coating was kept to 0.5 ± 0.1mm on each

173 face of the sample. The samples were grounded to powdered form to perform TGA as shown
174 in Figure 3c.



175

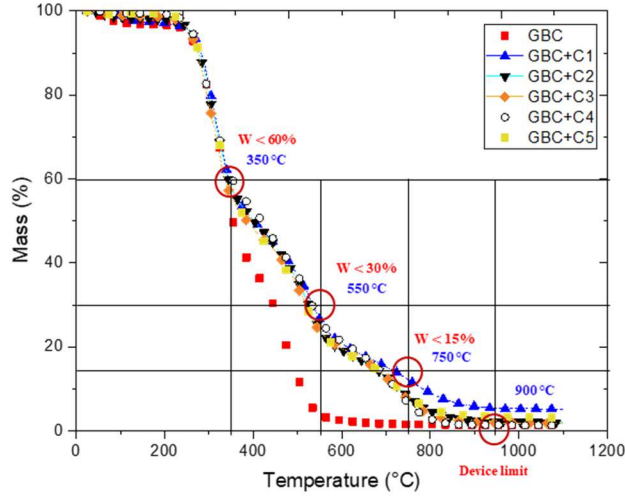
176 **Figure 3:** a) Controlled GBC, b) IFR coated GBC and c) Powdered form of sample

177 2.3. Thermogravimetric analysis

178 TG measures of the intumescent fire retardant (IFR) coated and uncoated green biocomposite
179 samples were performed using a TA instrument SDT Q600. A sample mass of 10-12 mg was
180 placed in platinum crucibles to perform thermal analysis in the range of 20-1100°C. In the
181 first stage of testing, controlled and all five types of IFR coated specimens were tested under
182 synthetic air at atmospheric pressure using 10°C/min. In the second stage of testing,
183 specimens from only the selected materials were placed in an inert and oxidative atmosphere.
184 The airflow rate was fixed to 100 ml/min and non-isothermal heating rates of 5, 10 and
185 15°C/min were used, which followed an isotherm of 5 min after reaching the final
186 temperature i.e. 1100°C before the cooling step.

187 2.4. Scanning electron microscopy

188 Scanning electron microscope (SEM) was used to analyse the morphology of the uncoated
189 (controlled) and fire retardant coated green biocomposite at four selected temperatures i.e.
190 350°C, 550°C, 750°C and 900°C. Temperatures selection was based on the decomposition
191 profile of the controlled and IFR coated green biocomposite as shown in Figure 4. The SEM
192 used to perform the morphological analysis was JEOL 7900 F. The samples were fixed with
193 double face carbon tape to perform the structural analysis.



194

195

Figure 4: Selection of temperature for performing morphological analysis

196

2.5. Energy dispersive spectroscopy

197

The energy dispersive spectroscopy (EDS) analyses was performed to carryout elemental analysis of the additives present in controlled and coated green biocomposite using a Bruker Flat Quad detector. The acceleration voltage was fixed to 4kV and other specifications, such as magnification, work distance were reported at the bottom of each image.

200

201

2.6. Kinetic analysis using theoretical model

202

Kinetics Neo software package developed by Netzsch Company was used to perform modelling and analysis of the degradation process of the samples. Opfermann has already discussed the principle but here we briefly discuss the basic concepts of the method again [34]. For making the kinetic analysis, it was assumed that decomposition of material takes place based on Equation 1.

206



207

The modelling of the kinetic decomposition of a green biocomposite was dependent on two functions, first one was dependent on temperature i.e. $k(T)$ and the second one was dependent on conversion rate (α) i.e. $f(\alpha)$. The conversion function, $f(\alpha)$ can vary from 0 to 1, which means that from zero degradation to complete degradation. Hence, the differential equation to define the kinetics of the process of thermal degradation can be written as Equation 2 [35].

211

$$\frac{d\alpha}{dt} = k(T)f(\alpha) \quad (2)$$

212 where $d\alpha/dt$ was the rate of degradation, $f(\alpha)$ stands for the reaction model, and $k(T)$ was the
 213 temperature dependent kinetic constant that was equal to Equation 3 according to Arrhenius
 214 law.

$$K(T) = A \exp\left(\frac{-E}{RT}\right) \quad (3)$$

215 where A , AE and R were the pre-exponential factor (1/s), activation energy (J/mol) and
 216 universal gas constant (J/K.mol) respectively [36]. The extent of conversion was determined
 217 as a fraction of total weight loss (Equation 3) [37], [38].

$$\alpha = \frac{m_i - m}{m_i - m_f} \quad (4)$$

218 where m_i , m_f and m were the initial, final and instantaneous mass of the sample respectively.
 219 The value of α denotes the transformation from the beginning (0) to completion (1).

220 To perform the kinetic analysis, it was assumed that all the reactions were irreversible since
 221 the gaseous emissions were continuously removed outside from the TA instrument during
 222 thermal degradation of the material. The overall reaction as mentioned in Equation 1 was the
 223 sum of all individual reaction steps with constant activation energy. Expanded Prout-Tompkins
 224 equation model, usually used for solid state kinetics, mentioned in Equation 4 was used to
 225 model the conversion function [39].

$$f(\alpha) = \alpha^m(1 - \alpha)^n \quad (5)$$

226 Isothermal heating runs were used to perform the kinetic analysis, therefore to eliminate the
 227 time dependency Equation 2 was divided by a constant heating rate i.e. $\beta = \frac{dT}{dt}$

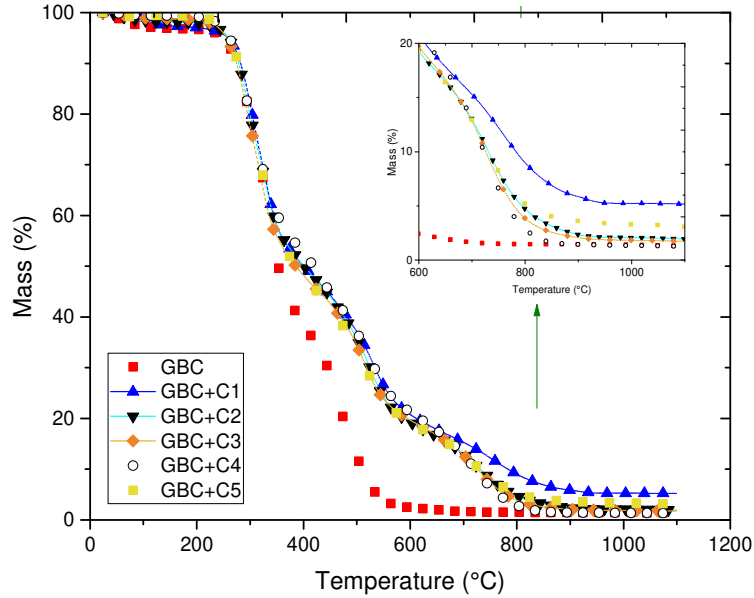
228 By doing the optimisation of model used for making the kinetic analysis, the kinetic
 229 parameters can be determined for each step in the process of thermal decomposition using
 230 Equation 6, and it would allow for a better understanding of the thermal degradation of the
 231 material.

$$\frac{d\alpha}{dT} = \frac{A}{\beta} \cdot e^{\left(\frac{-E}{RT}\right)} \cdot \alpha^m(1 - \alpha)^n \quad (6)$$

232

233 3. Results and discussion

234 TG curves of the thermal decomposition of controlled and fire retardant coated green
 235 biocomposite (GBC) under oxidative atmosphere at 10°C/min are presented in Figure 5.



236

237

Figure 5: TG curves of the thermal degradation of controlled and IFR coated green biocomposite

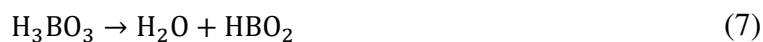
238

It is observed that the thermal degradation of GBC commenced at approximately 250°C and the material is completely degraded at 570°C. The detailed mechanism of the thermal degradation process of the newly developed GBC has been explained in a previous work by Rashid et al. [40]. To improve the thermal degradation profile of the newly developed biobased composite, five formulations having varying proportions of APP-THEIC and boric acid (mentioned in Table 1 of Section 2.2) were used in the form of surface coating. The fire retardant coating provides thermal protection to the GBC due to the formation of borophosphates between 250- 400°C [24]. Some research works have already explained the details of the protection mechanism of APP-THEIC and boric acid based coating [24], [41], [42].

248

Among the five tested formulations of fire retardant coating, the TG curves of GBC+C4, GBC+C3 and GBC+C2 shows similar pattern of decomposition. There seems to be no apparent difference to the level of protection provided by intumescent coating as the added mass percentage of boric acid is increased from 1wt.% to 3% and 5%. The fire retardant coating having even 1 wt.% of boric acid, as compared to only APP-THEIC containing coating, promotes the formation of carbonaceous char at high temperature due to decomposition of boric acid into metaboric acid (HBO_2) as shown in Equation 7, which eventually dehydrates, and leads to the formation of boron oxide (B_2O_3) as shown in equation 8. The glassy hard material, B_2O_3 , acts as thermally stable residue that provides a glue like adhesion to hold the char thus providing structural integrity to the material [24].

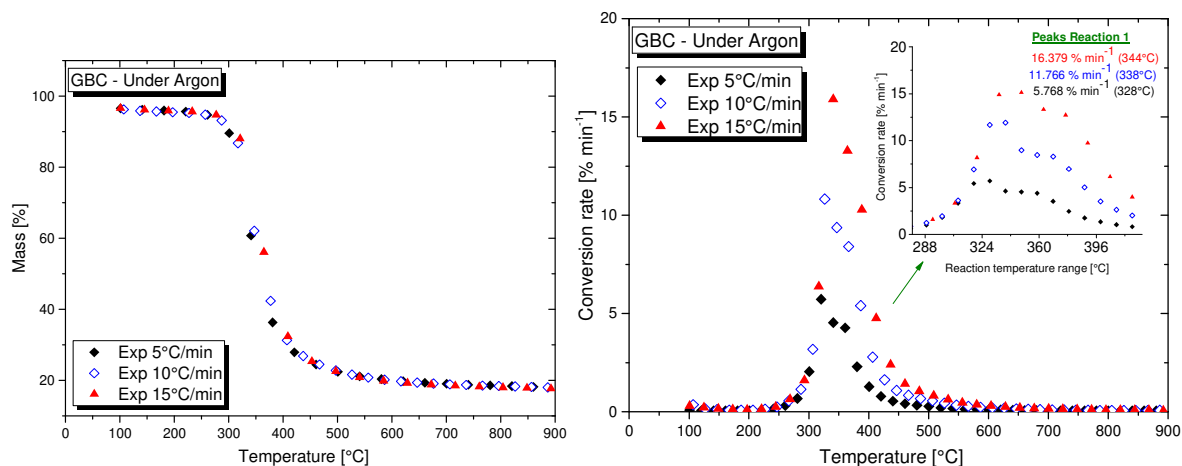
257



258 GBC+ C1 that had 10 wt.% of boric acid provides same level of thermal protection to GBC
 259 like other formulations until 660°C, however, after 660°C it displays reduced amount of
 260 thermal degradation with higher amount of residual char. Since the thermal degradation
 261 profiles of GBC+C4 and GBC+C1 displays unique behaviour as compared to other
 262 formulations, therefore further investigation on their thermal decomposition behaviour under
 263 inert and oxidative atmosphere at different heating rates was performed.

264 3.1. Thermal decomposition under inert atmosphere

265 TG curves and their corresponding derivative (DTG) curves of the thermal decomposition of
 266 green biocomposite at 5, 10 and 15 °C/min under argon are shown in Figure 6.

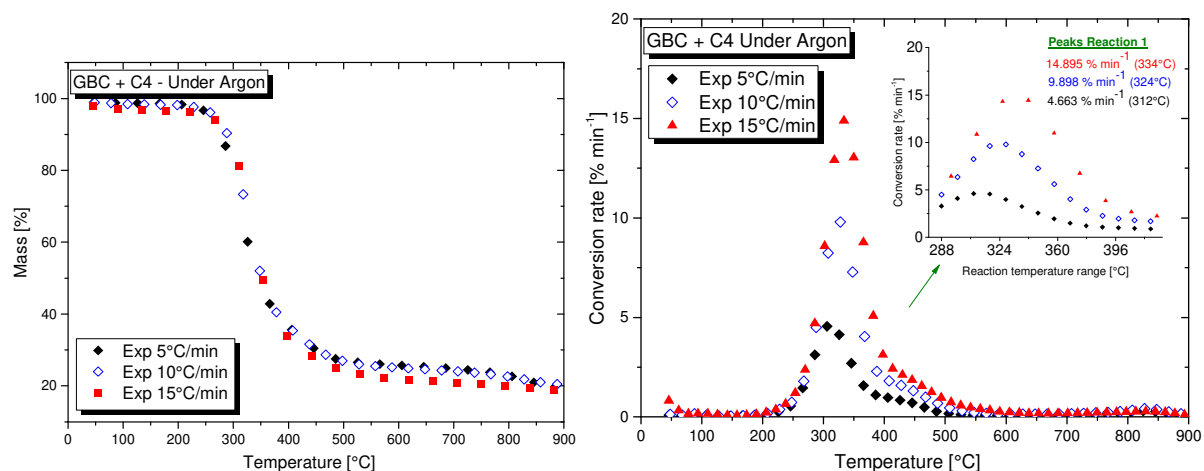


267
 268 **Figure 6:** Thermal decomposition of GBC under Argon at 5, 10 and 15°C/min

269 Green biocomposite shows a stable behaviour until 260°C under inert atmosphere of argon for
 270 all heating rates. The corresponding DTG curve shown in Figure 6 reveals that the
 271 temperature at the onset of decomposition stays same when the heating rate is increased. The
 272 TG curves shows a sharp mass loss step after the onset of decomposition, which corresponds
 273 to the DTG curve as a sharp peak. The maximum conversion rate, which results in a sharp
 274 mass loss step, occurs at 328°C for 5°C/min, 338°C for 10°C/min, 344°C for 15°C/min. The
 275 DTG curve shows that the rate of conversion doubles as the heating rate is doubled from
 276 5°C/min to 10°C/min and then to 15°C/min. It is observed on the TG and DTG curves under
 277 argon that the green biocomposite follows a one-step decomposition process.

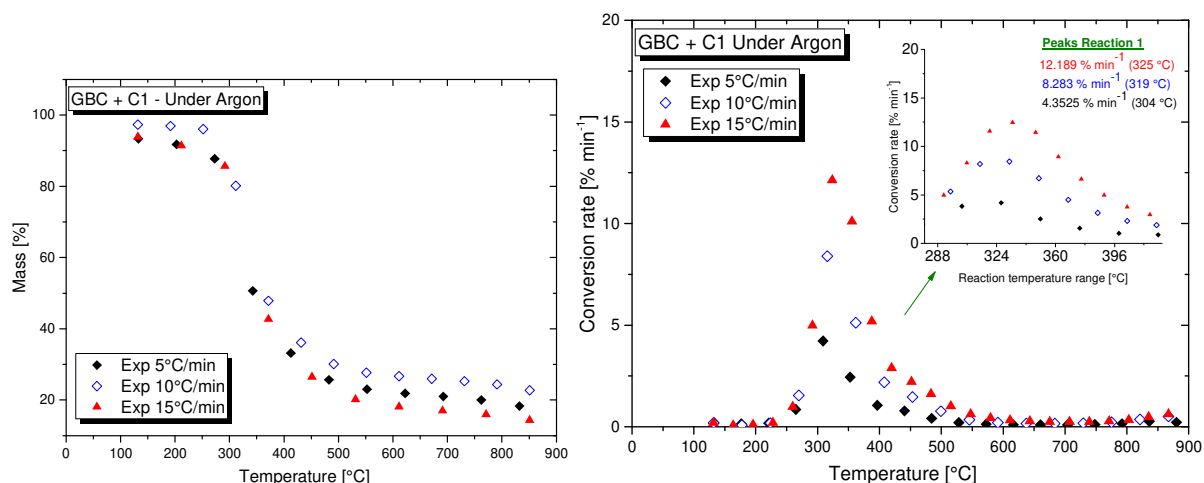
278 To gain an insight to improve the thermal decomposition profile of the green biocomposite,
 279 thermal degradation behaviour of GBC/29APP-TH/1BA (GBC+C4) and GBC/20APP-

280 TH/10BA (GBC+C1) at the three heating rates under inert atmosphere is studied. The TG and
 281 DTG curves of their thermal decomposition at 5°C/min, 10°C/min and 15°C/min under argon
 282 are displayed in Figure 7 and Figure 8.



283
 284

Figure 7: Thermal decomposition of GBC+C4 under Argon at 5, 10 and 15°C/min



285
 286

Figure 8: Thermal decomposition of GBC+C1 under Argon at 5, 10 and 15°C/min

287 It is observed on the TG curves of the thermal decomposition profile of the two fire retardant
 288 coated materials that they are exhibiting similar mass loss pathway as that of uncoated GBC.
 289 However, the onset decomposition temperatures of GBC/29APP-TH/1BA and GBC/20APP-
 290 TH/10BA are almost 20°C lower than that of GBC for all heating rates. This decrease in the
 291 onset decomposition temperature for the fire retardant coated green biocomposite can be
 292 attributed to the degradation of APP-THEIC that starts to degrade after 220°C to form
 293 phosphoric acid [24]. The peak temperature at the maximum rate of conversion is lower by
 294 10-15°C and 20-25°C for GBC/29APP-TH/1BA and GBC/20APP-TH/10BA respectively as
 295 compared to controlled GBC. The heating rates and their corresponding reaction temperatures
 296 are presented in Table 2.

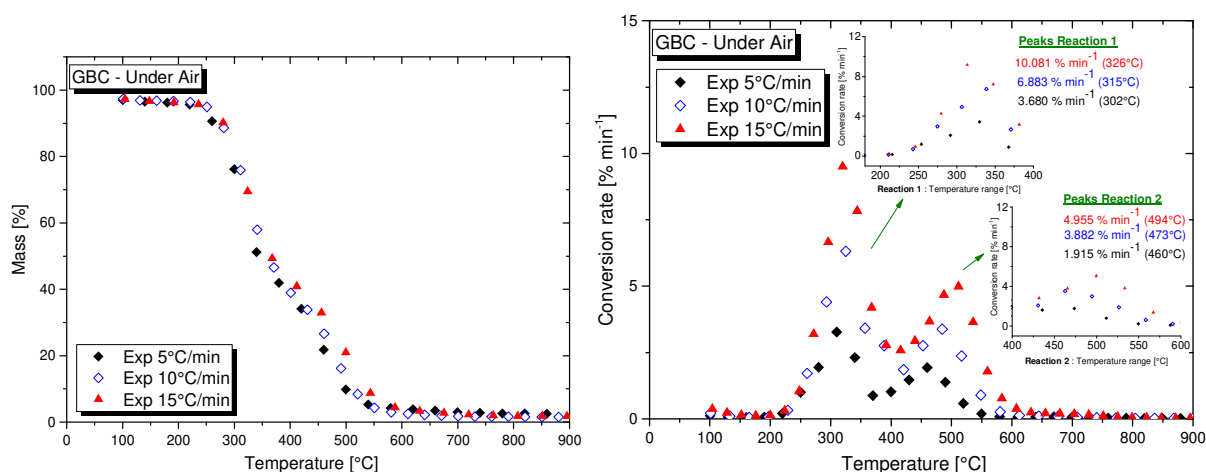
297 **Table 2:** Reaction temperatures for GBC, GBC+C1 and GBC+C4 associated with each peak determined from the DTG curves

β (C/min)	GBC Reaction 1 (°C)	GBC+C1 Reaction 1 (°C)	GBC+C4 Reaction 1 (°C)
5 °C/min	328	304	312
10 °C/min	338	31	324
15 °C/min	344	325	334

298

299 3.2. Thermal decomposition under oxidative atmosphere

300 The TG curves of the thermal decomposition of controlled green biocomposite exhibits a two-
 301 step decomposition process under oxidative atmosphere at the three heating rates, as shown in
 302 Figure 9. For the three heating rates i.e. 5, 10 and 15°C/min, the initiation of thermal
 303 decomposition of controlled GBC always takes place at 220°C and the maximum rate of
 304 decomposition, the main degradation step, is achieved at 302, 315 and 326°C respectively
 305 with almost 53% mass loss. After a slight stabilisation of few degrees of temperature, a
 306 second peak of mass loss was recorded. The two-step phenomenon is more visible on the
 307 DTG curves for all heating rates. At each heating rate, after the first peak of mass loss, there is
 308 a slight stabilization in conversion rate for few degrees before another peak of mass loss is
 309 recorded. The two-step phenomenon is visible on all heating rates. The DTG curves show the
 310 multi-step phenomenon clearer than the TG curves. It is evident on DTG curve that the first
 311 peak at 15°C/min is sharper as compared to others; this is of course due to higher heating rate
 312 that results in higher rate of conversion. It can be deduced from the TG and DTG curves
 313 under different heating rates that the thermal decomposition of green biocomposite occurred
 314 with at least two thermal decomposition steps under air.



315

316 **Figure 9:** Thermal decomposition of GBC under Air at 5, 10 and 15°C/min

317 The IFR coating on green biocomposite reduces the initial decomposition temperature (IDT)
 318 by 20°C, most likely due the addition of boric acid and APP-THEIC (Table 3).

319 **Table 3:** Initial and peak decomposition temperature of thermal decomposition of GBC, GBC+C4 and GBC+C1

Samples	°C/min	IDT	T _{max} (°C)		
			Reaction 1	Reaction 2	Reaction 3
GBC	5	220	302	460	-
	10	220	315	473	-
	15	220	326	494	-
GBC+C4	5	200	285	489	702
	10	200	296	516	728
	15	200	306	534	757
GBC+C1	5	200	287	481	635
	10	200	301	513	702
	15	200	311	527	748

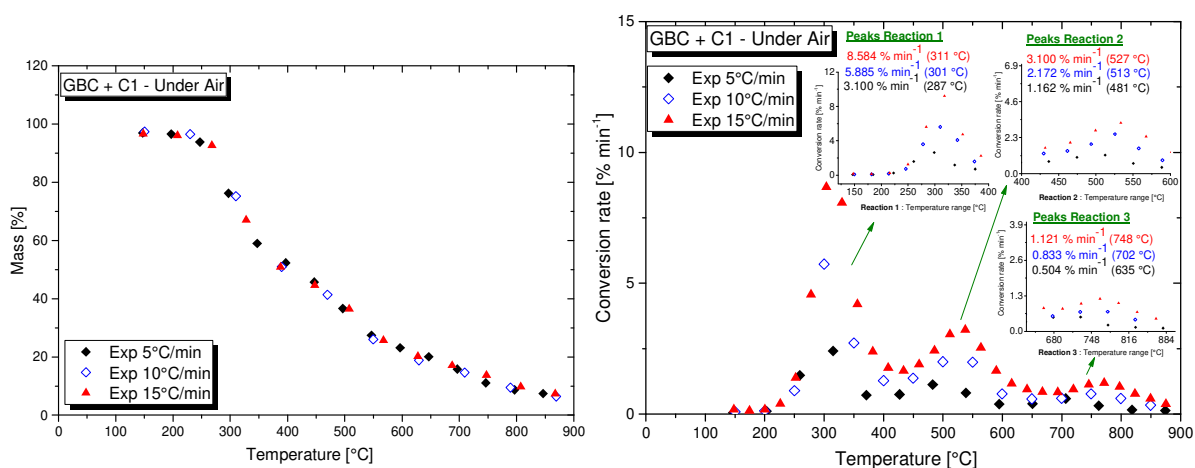
320

321 The first peak of decomposition for GBC+C4 and GBC+C1 reaches 17°C and 19°C earlier
 322 then the main degradation peak of GBC as shown in Figure 10 and Figure 11. This might be
 323 due to the decomposition of APP-THEIC occurring at 200°C; resulting in the formation of
 324 phosphoric acid. Until 140°C, boric acid is converting to boron oxide (Equation 9), and APP-
 325 THEIC is converting into phosphoric acid at 200°C (Equation 10), so a possible reaction
 326 between boron oxide and phosphoric acid results in the formation of borophosphates at
 327 approximately 250-400°C (Equation 11). The development of borophosphates forms an
 328 efficient intumescent system [24].

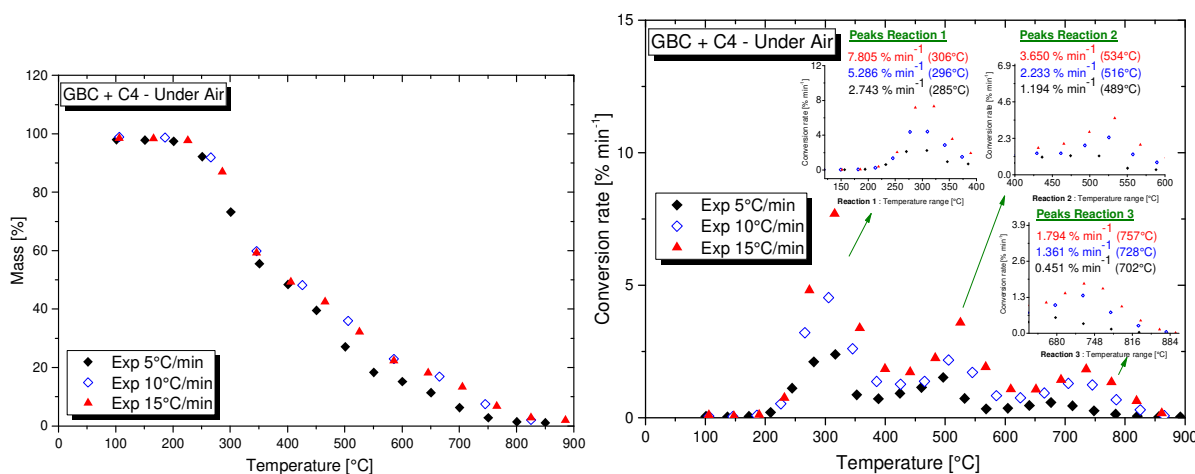


329 The largest peak of degradation in Figure 9 for each heating rate between 300 and 400°C
 330 corresponds to the degradation of green biocomposite. After 400°C, there is a slight
 331 stabilisation in temperature and further decomposition of the material takes place at higher
 332 temperature as compare to the decomposition of controlled green biocomposite. Further
 333 degradation of GBC due to evolution of volatiles and the oxidation of char layer results in the
 334 second peak, which appears at 460, 473 and 494 °C for the three heating rates respectively.

335 As compared to the GBC, the second peak of the decomposition of GBC+C4 and GBC+C1
 336 appears at a higher temperature. The reason behind this delay in degradation of IFR coated
 337 GBC is the presence of hard glassy fire protective coating of borophosphates on fire retardant
 338 coated GBC. The DTG curves displays that the complete degradation of GBC takes place at
 339 around 660°C. However, the fire retardant coated GBC continues to degrade and a third peak
 340 appears on the DTG curve. A thermal decomposition comparison between GBC+C4 and
 341 GBC+C1 reveals that GBC+C4 provides better protection to the material against thermal
 342 decomposition than GBC+C1. Especially the third peak of thermal decomposition of
 343 GBC+C4, where the oxidation of the formed char layer is taking place, provides reduced
 344 thermal degradation rate.



345
 346 **Figure 10:** Thermal decomposition of GBC+C1 under Air at 5, 10 and 15°C/min



347
 348 **Figure 11:** Thermal decomposition of GBC+C4 under Air at 5, 10 and 15°C/min

349 3.3. Kinetic analysis

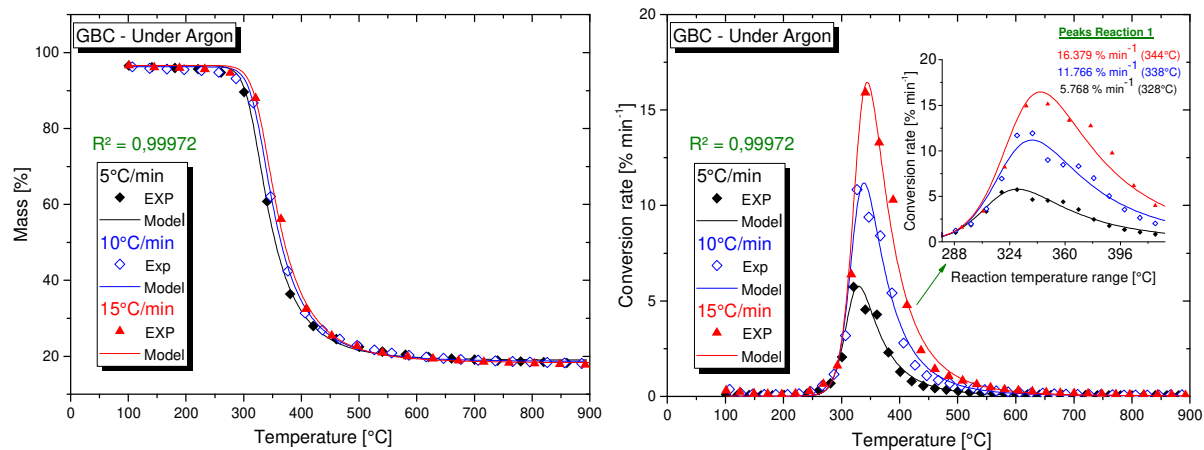
350 The kinetic analysis of the processes taking place in the green biocomposites, that are made-
 351 up of polymeric materials and natural fibres, starts from thermo-analytical measurements. In

352 thermo-analytical investigation the measured signal changes with the course of chemical
 353 processes and reflects the kinetic nature of the changes taking place in the process [43]–[46].
 354 Therefore, it is mandatory to carry out several measurements at different heating rates [34],
 355 [45]. Since the mechanism of degradation of composite materials are often complicated and
 356 multi-stepped, therefore two complementary methods i.e. model free and reaction model fit
 357 have been developed to determine fundamental kinetic parameters [47], [48]. Model-free
 358 methods are used for quick calculations and provide useful information for model based
 359 analysis. Model free methods, such as isoconversional approach is usually sufficient for single
 360 step processes only, since they do not consider the relationship among various steps involved
 361 so only one value of activation energy can be determined. Whereas to determine the pre-
 362 exponential coefficient, it is essential to undertake the provision of the conversion function
 363 i.e. $f(\alpha)$ [44], [45]. Thus, model-free methods are not suitable for characterizing complex
 364 phenomenon in competitive reactions that were dependent on heating rates [44], [48].
 365 Therefore, a number of kinetic models were suggested in the course of research work based
 366 on the type of reactions. The kinetic models and the selected form of functions are
 367 summarised in Table 4.

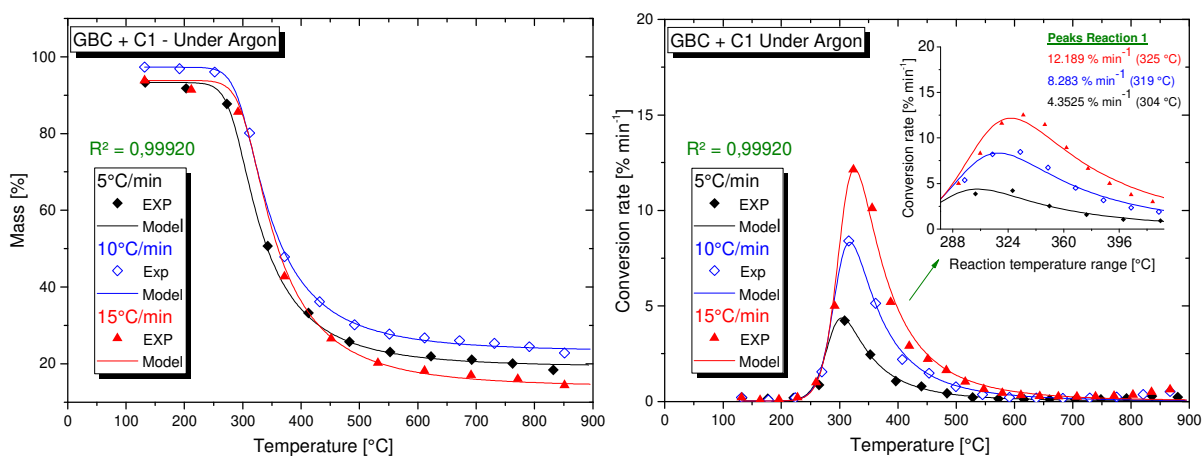
368 **Table 4:** Reaction types and corresponding reaction equations

Code	Function	Type of Reaction
F1	$f = (1 - \alpha)$	Reaction of 1st order
F2	$f = (1 - \alpha)^2$	Reaction of 2nd order
F _n	$f = (1 - \alpha)^n$	Reaction of nth order
R2	$f = 2(1 - \alpha)^{1/2}$	Two-dimensional phase boundary
R3	$f = 3(1 - \alpha)^{2/3}$	Three-dimensional phase boundary
D1	$f = 1/2 \cdot 1/\alpha$	One-dimensional diffusion
D2	$f = -1/\ln((1-\alpha))$	Two-dimensional diffusion
D3	$f = 3/2 \cdot (1-\alpha)^{2/3}/1-(1-\alpha)^{1/3}$	Three-dimensional diffusion Jander's type
D4	$f = 3/2 \cdot 1/((1-\alpha) -^{1/3} - 1)$	Three-dimensional diffusion Ginstling–Brounstein type
B1	$f = (1 - \alpha) \cdot \alpha$	Prout–Tompkins equation
B _{na}	$f = (1 - \alpha)^n \cdot \alpha^{K_{cat}}$	Expanded Prout–Tompkins equation
C1	$f = (1 - \alpha) \cdot (1 + K_{cat} \cdot \alpha)$	Reaction of 1st order with autocatalyswas by product
C _n	$f = (1 - \alpha)^n \cdot (1 + K_{cat} \cdot \alpha)$	Reaction of nth order with autocatalyswas by product
C _{nm}	$f = (1 - \alpha)^n \cdot (1 + K_{cat} \cdot \alpha^m)$	Reaction of nth order with m-Power autocatalyswas by product
A2	$f = 2(1 - \alpha) \cdot [-\ln(1 - \alpha)]^{1/2}$	Two-dimensional nucleation according to Avrami
A3	$f = 3(1 - \alpha) \cdot [-\ln(e)]^{2/3}$	Three-dimensional nucleation according to Avrami

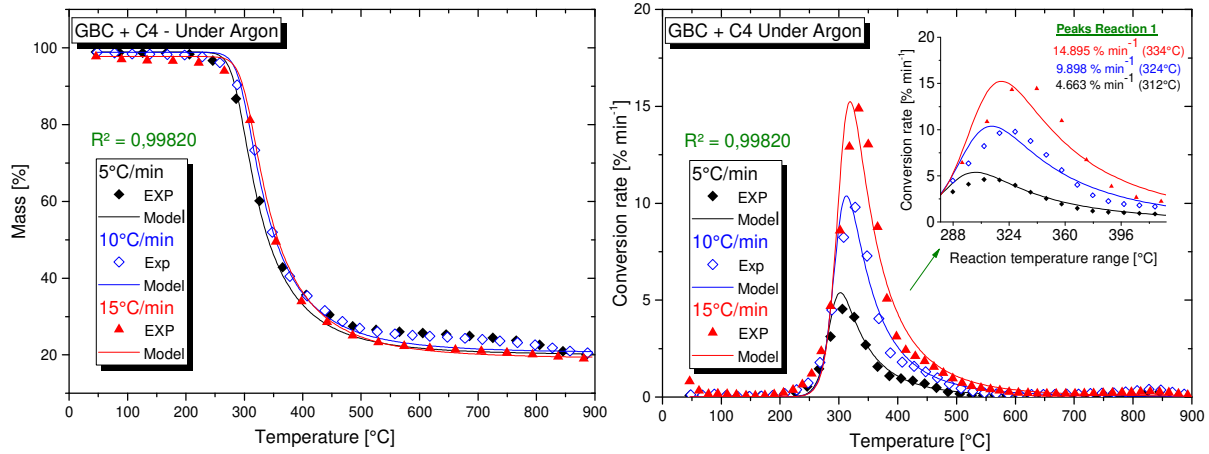
369 To determine kinetic parameters and to obtain significant information on the mechanism of
 370 the degradation process, model-based analysis was carried out. The thermal decomposition
 371 data of GBC, GBC+C1 and GBC+C4 under inert and oxidative atmosphere carried out at the
 372 three heating rates was fitted on Expanded Prout–Tompkins solid-state reaction model using
 373 Netzsch thermokinetics to determine the kinetic parameters. Expanded Prout–Tompkins
 374 (Bna) model fits the original data of thermal decomposition under inert and oxidative
 375 atmosphere with a high correlation coefficient of 0.99972 as shown in Figure 12 and Figure
 376 13, which confirms the reliability and accuracy of obtained values of kinetic parameters. The
 377 kinetic triplets estimated using this method were presented in Table 5 and Table 6.



378



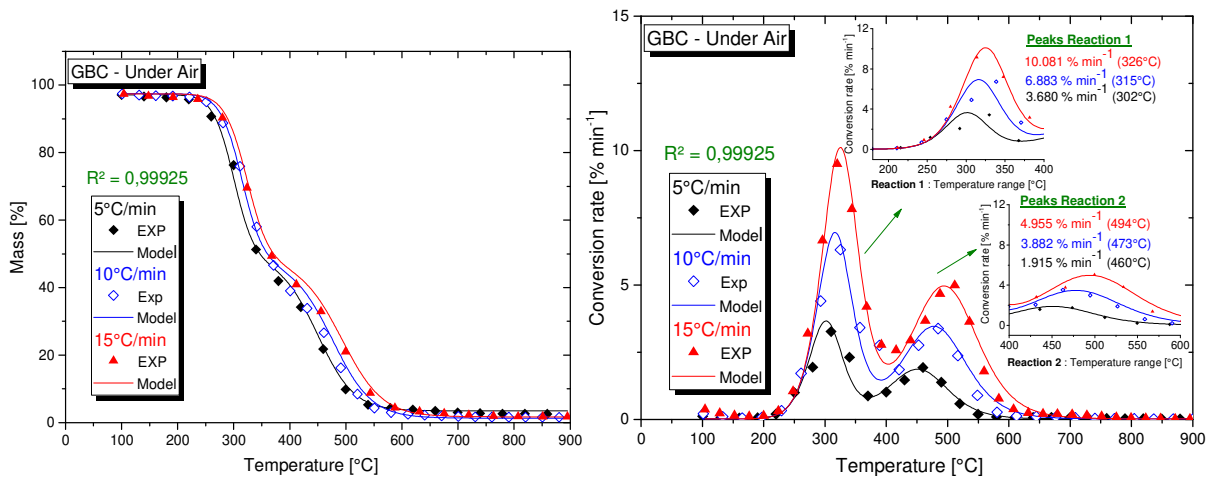
379



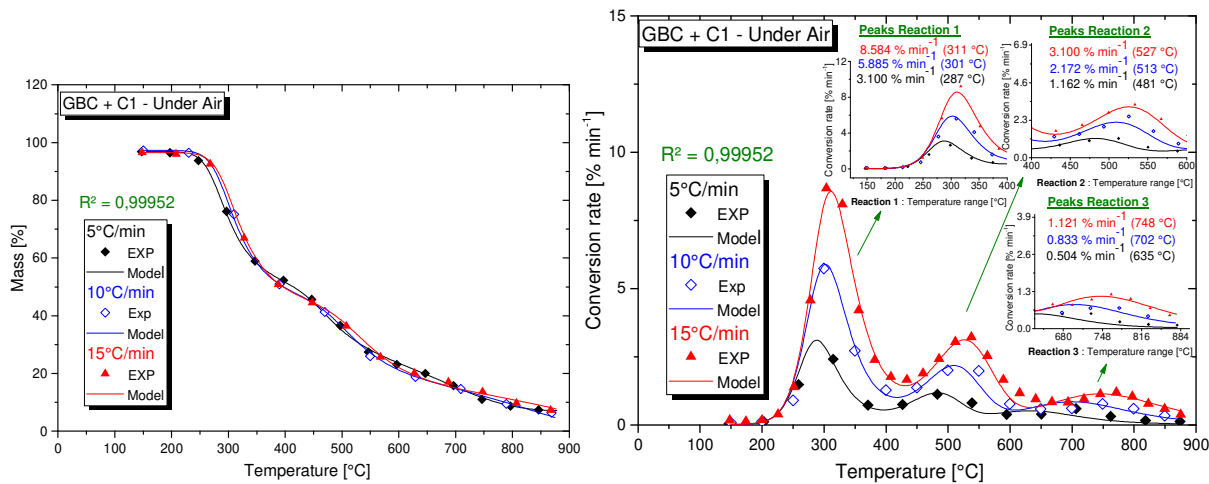
380

381

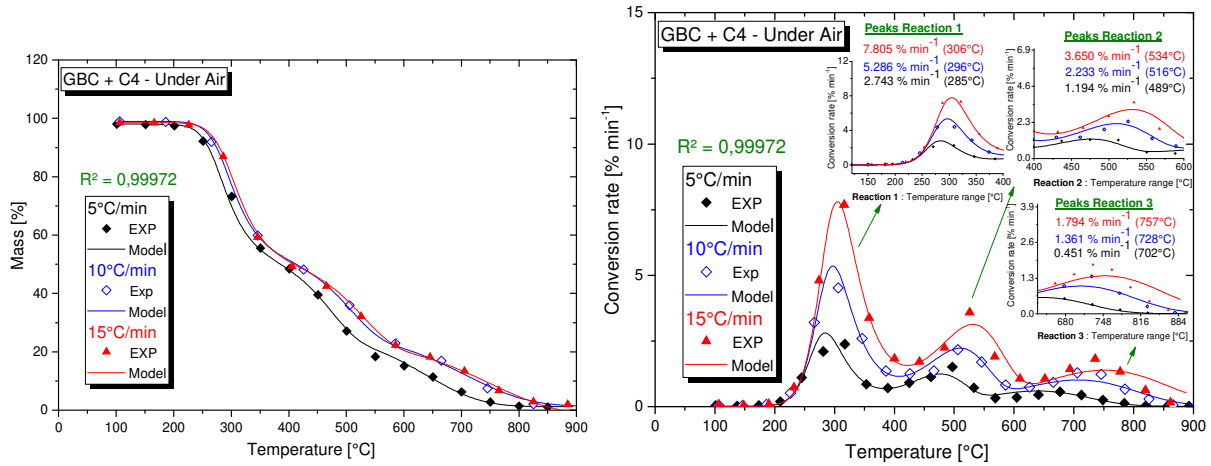
Figure 12: TGs and their corresponding DTGs of GBC, GBC+C1, GBC+C4 under inert atmosphere



382



383



384

385

Figure 13: TGs and their corresponding DTGs of GBC, GBC+C1, GBC+C4 under oxidative atmosphere

386

It should be noted that approximately 100% conversion has been achieved for GBC, which means that whole of the material has decomposed. This hypothesis is verified by seeing the DTG almost constant at 600°C, therefore it could be ascertained that the conversion is nearly 100% at that temperature for the corresponding step of decomposition

387

388

389

Table 5: Kinetic parameters of thermal decomposition of GBC, GBC+C1 and GBC+C4 under inert atmosphere

Parameters	GBC	GBC+C4	GBC+C1
E [kJ/mol]	216,250	176,216	135,478
Log (A) [Log(1/s)]	16,518	13,804	9,925
n [-]	4,304	4,969	4,519
m [-]	0,01	0,217	0,190

390

391

Table 6: Kinetic parameters of thermal decomposition of GBC, GBC+C1 and GBC+C4 under inert atmosphere

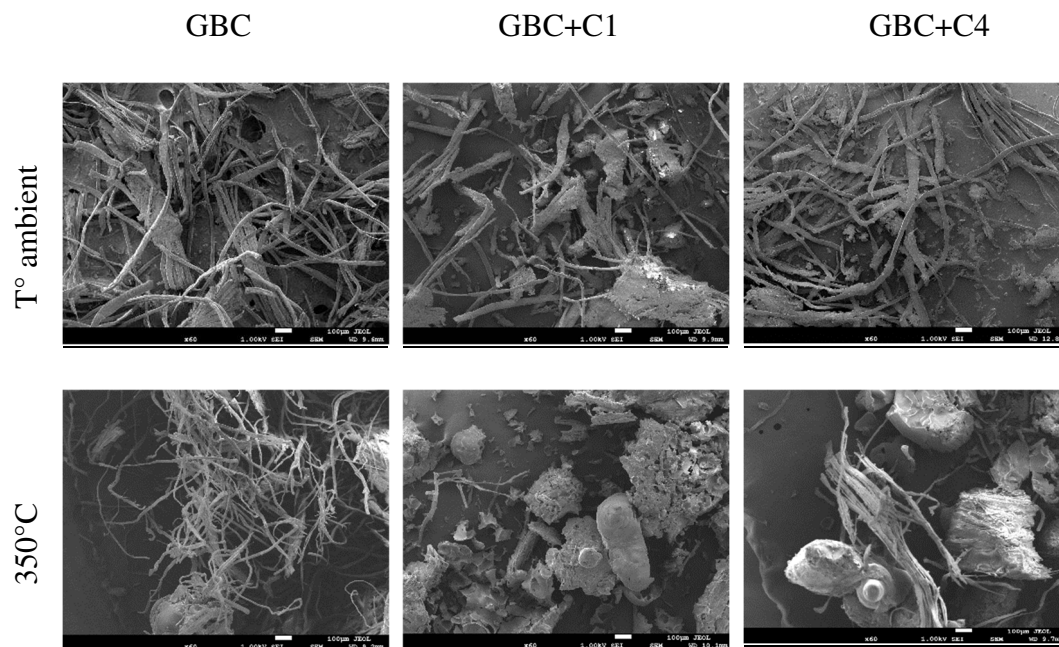
	GBC	GBC+C4	GBC+C1
E ₁ [kJ/mol]	122,953	133,784	133,639
Log (A ₁) [Log(1/s)]	8,774	10,171	10,115
n ₁ [-]	1,699	2,920	3,648
m ₁ [-]	0,01	0,01	0,134
E ₂ [kJ/mol]	104,902	84,634	76,425
Log (A ₂) [Log(1/s)]	4,864	3,146	2,810

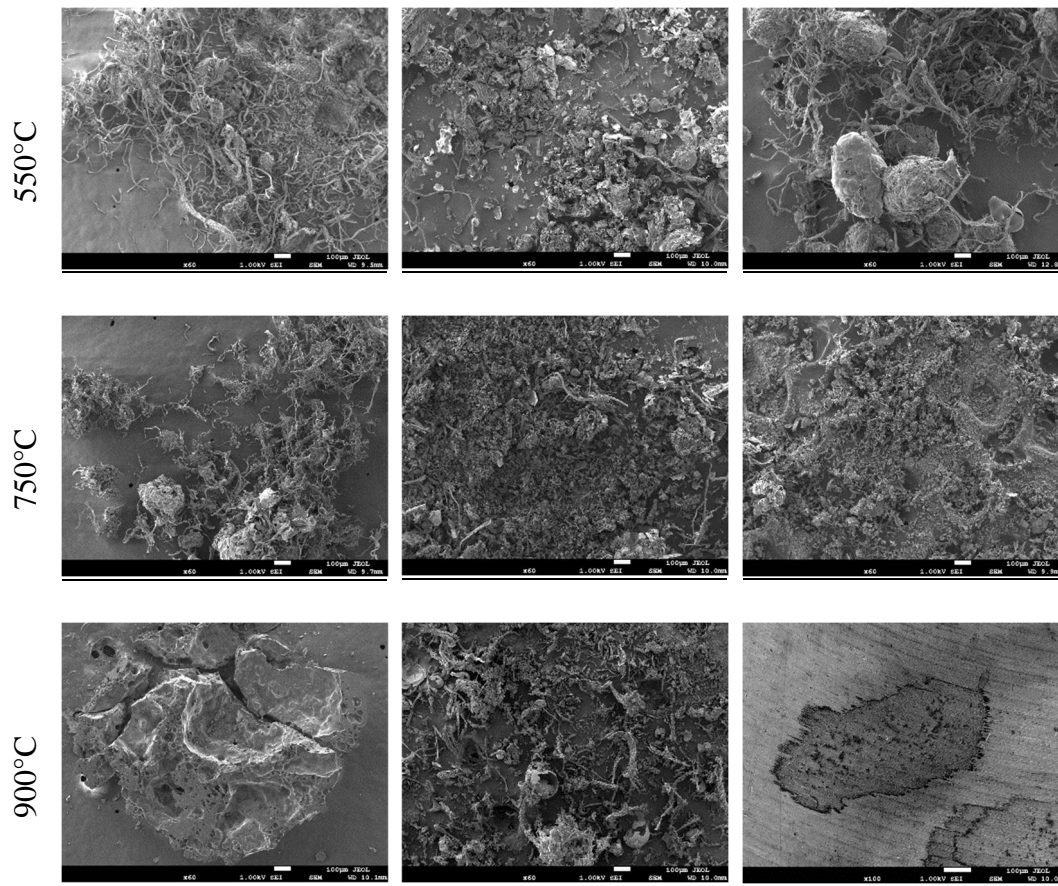
	n_2 [-]	1,593	0,889	2,512
	m_2 [-]	0,01	0,01	0,416
Reaction 3	E_3 [kJ/mol]		60,290	18,217
	Log (A_3) [Log(1/s)]	-	0,422	0,357
	n_3 [-]		0,965	1,449
	m_3 [-]		0,143	0,399

393 The activation energy of a thermal decomposition processes can be used as criteria for making
 394 a comparison about the thermal stability of polymeric composites [49].

395 3.4. Morphological analysis

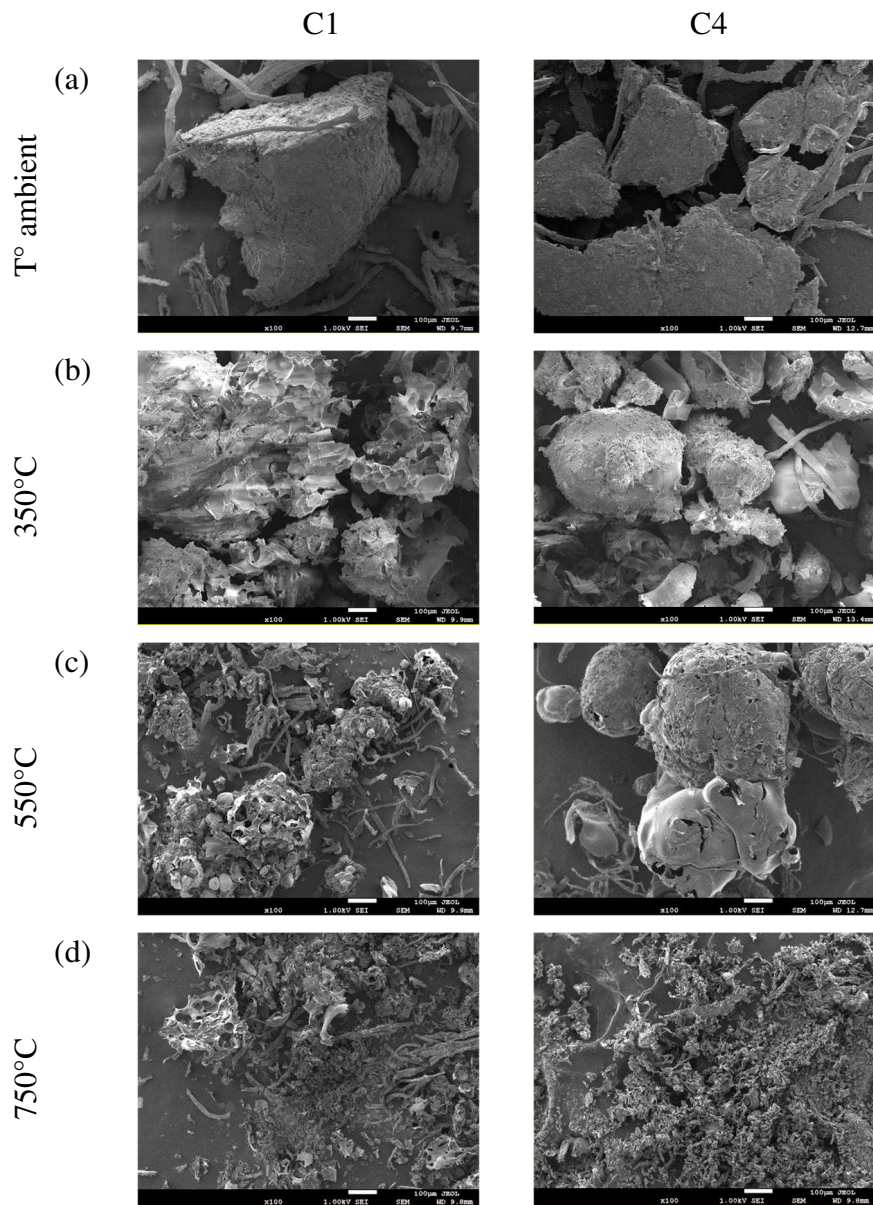
396 Microscopic analysis of the thermally degraded uncoated and coated green biocomposite with
 397 intumescent fire retardant coating i.e. C1 and C4 were executed with the scanning electron
 398 microscope (SEM) to examine and analyse the morphology of the thermally degraded
 399 materials (GBC+C1 and GBC+C4). The SE micrographic images of the
 400 thermogravimetrically-analysed samples at four selected temperatures are shown in Figure 14.

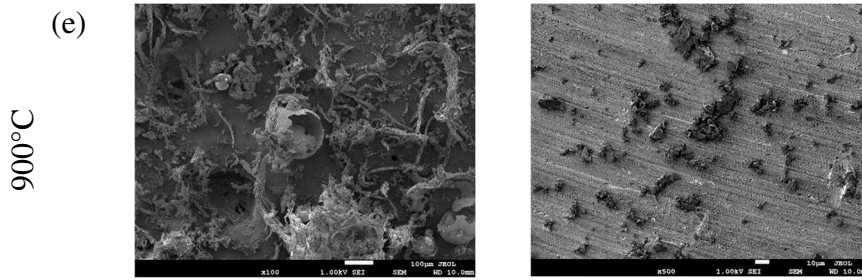




401 **Figure 14:** SEM images of thermally decomposed GBC, GBC+C1 and GBC+C4 at 350, 550, 750, and 900°C
 402 In Figure 15, enhanced images focused on IFR coating are presented. It is evident in the
 403 images that the fire retardant coating, comprised of APP-THEIC and boric acid, forms an
 404 intumescent fire protective coating to protect the material against thermal exposure. It has
 405 been explained in Section 3.2 that APP-THEIC and boric acid reacts between 250-400°C to
 406 form borophosphate that forms a protective coating on the surface of materials. Figure 15b
 407 reveals the morphology of the fire protective coating, where cracked microstructure can be
 408 seen on the surface of C1 at 350°C. The presence of cracks in protective coating illustrates
 409 partial protection and the bigger pore would promote heat transfer to the substrates,
 410 consequently resulting in higher substrate temperatures [13]. The cracks and holes also
 411 provide an escape to combustible volatiles thus adding fuel to the fire. The outer surface of
 412 C4 in Figure 15b at 350°C shows a compact surface with fewer cracks. There were many
 413 irregular small holes of the soft foam in the charring layer due the dehydration of APP and
 414 boric acid in the range of relatively suitable temperature. The formation of the bubbles is due
 415 to the emission of CO₂ and NH₃ gases, which bubbles through the viscous liquid and expands
 416 the char formed. The char layers of the intumescent formulation act as a fire-resistant layer,

417 provide heat insulation and, thus shields the underlying green biocomposite substrate [50]. As
418 the temperature was further increased to 550°C, the thermal protective coating provided by
419 C1 fails (Figure 15); however, C4 continues to provide thermal protection to the material but
420 with reduced efficiency due to the formation of larger cracks on the surface of coating. The
421 phenomenon of the failure of intumescent coating having 20wt% APP-THEIC and 10wt%
422 boric acid (C1) can be attributed to the higher percentage of boric acid that act as a blowing
423 agent.

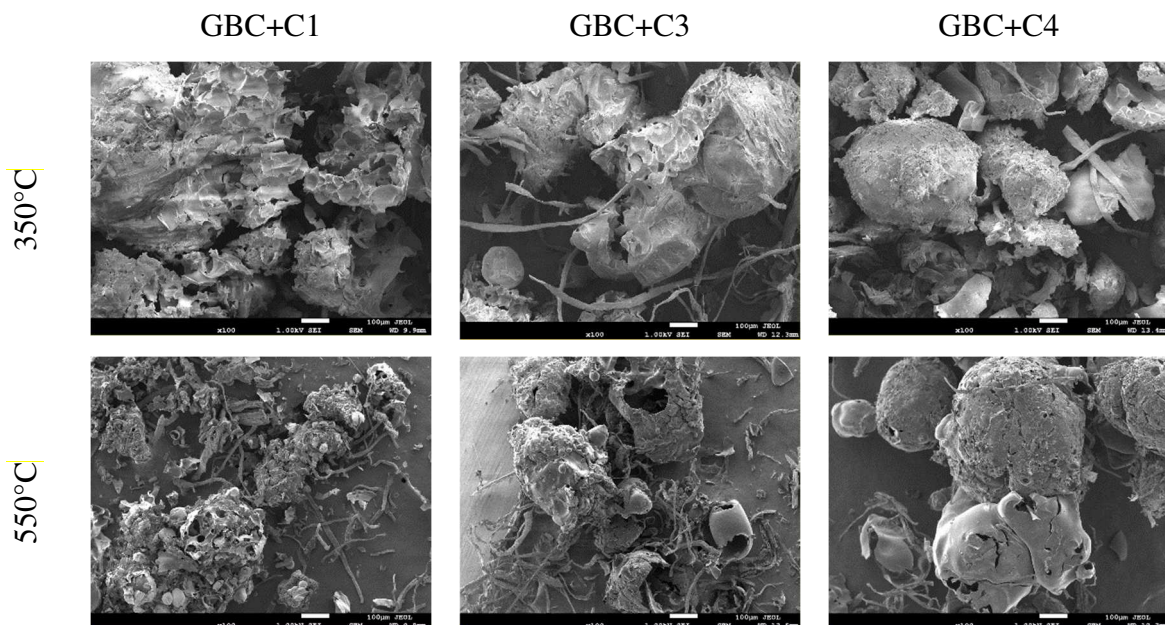




424 **Figure 15:** Focused SEM images of thermally decomposed GBC+C1 and GBC+C4 at 350, 550, 750, and 900°C

425 To investigate the effect of the percentage of boric acid, C3 that had 27wt.% of APP-THEIC
 426 and 3wt.% boric was examined at 350°C and 550°C as shown in Figure 16. It can be observed
 427 in the micrographs that as the amount of boric acid is increased the quality of IFR coating
 428 degenerates due to presence of excessive quantity of blowing agent that result into
 429 disproportionate dehydration, and escape of volatiles and gaseous compounds. At 750°C, the
 430 material is devoid of any thermal protection and only residual char is left.

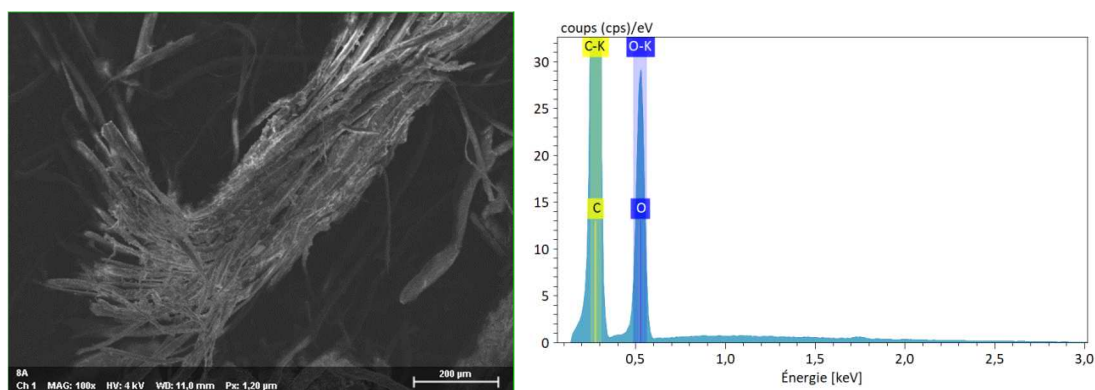
431 The residual mass of GBC+C1 is indeed higher as compared to GBC+C4 due the presence of
 432 higher amount of boric acid that does not fully degrade due its intrinsic nature. In terms of
 433 residual mass, GBC+C1 always leaves a residual mass as shown in Figure 15d, but this
 434 cannot be the criteria of better thermal protection while testing IFR coating. The
 435 morphological analysis of the selected coatings reveals that GBC+C4 provides better thermal
 436 protection since the expansion and structure of the char are very vital to fire-retardant
 437 properties of coatings [51].



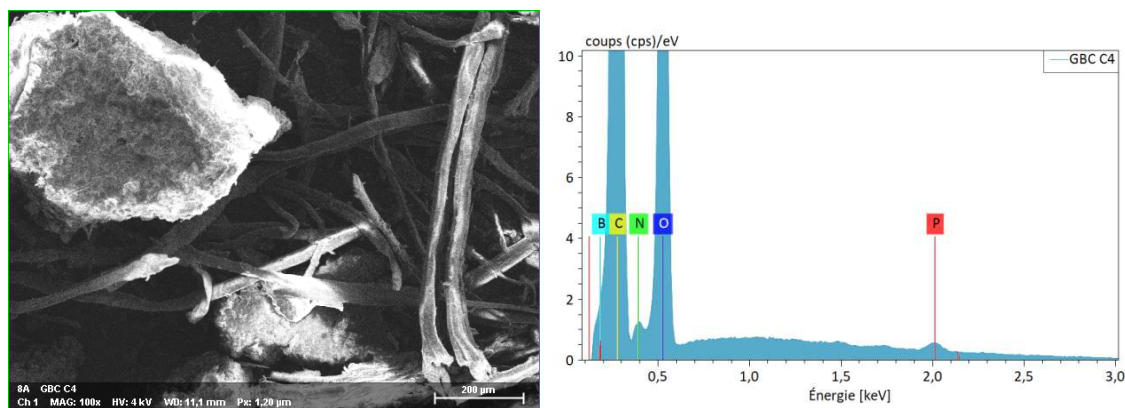
438 **Figure 16:** SEM images of thermally decomposed GBC+C1, GB+C3, and GBC+C4 at 350, 550°C

439 3.5. Elemental analysis of the coated and uncoated material

440 The energy dispersive X-ray spectroscopy (EDS) of the specimens of GBC reveals the
441 presence of carbon and oxygen in Figure 17. The peaks of carbon and oxygen can be
442 attributed to the presence of carbon and oxygen in flax and epoxy. The ED spectroscopy of
443 green biocomposite coated with C4 (Epoxy, 29wt.%APP and 1wt.%BA) exposes the
444 presence of boron, carbon, nitrogen, oxygen, and phosphorous in Figure 18. The carbon peak
445 is again due to flax fibre and epoxy, whereas the peak of oxygen comes from flax, epoxy,
446 APP, and boric acid. The peaks of nitrogen and phosphorous are due to the presence of
447 ammonium polyphosphate (APP) and boron peak comes from boric acid.



448
449 **Figure 17:** SEM image and corresponding EDS spectrum of green biocomposite



450
451 **Figure 18:** SEM image and corresponding EDS spectrum of GBC/29APP/1BA

452 **4. Conclusion**

453 The thermal degradation of a green biocomposite coated with an IFR coating is investigated
454 and explained using thermo-chemical reactions and kinetic analysis. The application of fire
455 retardant coating having APP-THEIC and boric acid improves fire retardant properties of the
456 green biocomposite due to the formation of borophosphates, which is responsible for the
457 development of a glassy hard intumescent char. However, determination of optimum
458 proportions of each component that can produce an efficient coating remains a major

459 challenge. In this regard, among the TGA analysis of all specimens GBC+C1 that was coated
460 with E/20APP-THEIC/10BA and GBC + C4 that was coated with E/29APP-THEIC/1BA
461 displayed better performance. They exhibited similar thermal degradation profiles in TGA but
462 thermal degradation of E/20APP-THEIC/10BA results in higher amount of residual char.
463 Since higher amount of residual char could not be ascertained as the final criterial of efficient
464 intumescent fire retardant coating therefore scanning electron microscopy was also carried out
465 to gain more clarity about efficiency of the protective coating. SEM analysis reveals better
466 morphology and integral structure of the material when E/29APP-THEIC/1BA was used. To
467 perform kinetic analysis, Expanded Prout–Tompkins solid-state reaction equation was used to
468 model the thermal degradation behaviour of the coated green biocomposite under inert and
469 oxidative conditions, and we have shown a very good agreement between experimental and
470 modelled curves at different heating rates. This approach allows us to evaluate the thermal
471 degradation behaviour of a material in fire scenario, and when this method was used in
472 conjunction with other small-scale tests, it allows us to avoid carrying out full-scale expensive
473 and time-consuming tests.

474 Nomenclature

475	Ammonium polyphosphate	APP
476	Boric acid	BA
477	Energy dispersive spectroscopy	EDS
478	Epoxy	E
479	Flame retardant	FR
480	Green biocomposite	GBC
481	Intumescent flame retardant	IFR
482	Thermogravimetric analysis	TGA
483	Tris (2- hydroxyethyl) isocyanurate	THEIC
484	Scanning electron microscope	SEM

485 **Author's contribution**

486 **Madiha RASHID:** Conceptualization, methodology, software, validation, formal analysis,
487 investigation, writing original draft, writing review and editing, visualization. **Khaled**
488 **CHETEHOUNA:** Conceptualization, resources, supervision, project administration, funding

489 acquisition, validation. **Abdelhakim SETTAR:** Software, Validation, formal analysis,
490 writing review and editing. **Julie ROUSSEAU:** Methodology, investigation. **Christelle**
491 **ROUDAUT:** Investigation. Laurent LEMEE: Methodology, writing review and editing.
492 **Zoheir ABOURA:** Validation, resources.

493 **Funding**

494 This work was supported by the Higher education commission of Pakistan.

495 **Competing interests**

496 The authors declare that they have no competing interests.

497 **References**

- 498 [1] R. Vinayagamoorthy and I. V Manoj, “Natural fiber for green technology in
499 automotive industry : A brief review Natural fiber for green technology in automotive
500 industry : A brief review,” 2018.
- 501 [2] E. Zini and M. Scandola, “Green Composites : An Overview,” *Polym. Compos.*, pp.
502 1905–1915, 2011.
- 503 [3] F. M. Al-Oqla and M. A. Omari, “Sustainable biocomposites: Challenges, potential and
504 barriers for development,” *Green Energy Technol.*, pp. 13–29, 2016.
- 505 [4] M. Rashid, K. Chetehouna, A. Cablé, and N. Gascoin, “Analysing Flammability
506 Characteristics of Green Biocomposites: An Overview,” *Fire Technol.*, vol. 57, no. 1,
507 pp. 31–67, 2021.
- 508 [5] Y. Chen, O. Chiparus, L. Sun, I. Negulescu, D. V Parikh, and T. A. Calamari, “Natural
509 Fibers for Automotive Nonwoven Composites,” *J. Ind. Text.*, vol. 35, no. 1, 2005.
- 510 [6] J. Holbery and D. Houston, “Natural-Fiber-Reinforced Polymer Composites in
511 Automotive Applications,” *JOM*, vol. 58, no. 11, pp. 80–86, 2006.
- 512 [7] S. N. Monteiro, F. P. D. Lopes, A. S. Ferreira, and D. C. O. Nascimento, “Natural-fiber
513 polymer-matrix composites: Cheaper, tougher, and environmentally friendly,” *JOM*,
514 vol. 61, no. 1, pp. 17–22, 2009.
- 515 [8] T. H. Nam, S. Ogihara, and S. Kobayashi, “Interfacial , Mechanical and Thermal
516 Properties of Coir Fiber-Reinforced Poly (Lactic Acid) Biodegradable Composites,”
517 *Adv. Compos. Mater.*, vol. 21, no. February, pp. 103–122, 2012.

- 518 [9] D. Price, G. Anthony, and P. Carty, "1 - Introduction: polymer combustion, condensed
519 phase pyrolysis and smoke formation," in *Fire Retardant Materials*, A. R. Horrocks
520 and D. Price, Eds. Woodhead Publishing, 2001, pp. 1–30.
- 521 [10] H. Vandersall, "Intumescent coating system, their development and chemistry," 1971.
- 522 [11] J. A. Rhys, "Intumescent coatings and their uses," *Fire Mater.*, vol. 4, no. 3, pp. 154–
523 156, Sep. 1980.
- 524 [12] M. Bar, A. Ramasamy, and A. Das, "Flame Retardant Polymer Composites," *Fibres*
525 *Polym.*, vol. 16, pp. 705–717, Nov. 2014.
- 526 [13] S. Duquesne, S. Magnet, C. Jama, and R. Delobel, "Intumescent paints: fire protective
527 coatings for metallic substrates," *Surf. Coatings Technol.*, vol. 180–181, pp. 302–307,
528 2004.
- 529 [14] J. H. Koo, W. Wootan, W. K. Chow, H. W. Au Yeung, and S. Venumbaka,
530 "Flammability Studies of Fire Retardant Coatings on Wood," in *Fire and Polymers*,
531 vol. 797, American Chemical Society, 2001, pp. 28–361.
- 532 [15] G. Camino, L. Costa, and G. Martinasso, "Intumescent fire-retardant systems," *Polym.*
533 *Degrad. Stab.*, vol. 23, no. 4, pp. 359–376, 1989.
- 534 [16] A. R. Horrocks, "Developments in flame retardants for heat and fire resistant textiles—
535 the role of char formation and intumescence," *Polym. Degrad. Stab.*, vol. 54, no. 2, pp.
536 143–154, 1996.
- 537 [17] R. Delobel, M. Le Bras, N. Ouassou, and F. Alistiqsa, "Thermal Behaviours of
538 Ammonium Polyphosphate-Pentaerythritol and Ammonium Pyrophosphate-
539 Pentaerythritol Intumescent Additives in Polypropylene Formulations," *J. Fire Sci.*,
540 vol. 8, no. 2, pp. 85–108, Mar. 1990.
- 541 [18] G. Camino, G. Martinasso, and L. Costa, "Thermal degradation of pentaerythritol
542 diphosphate, model compound for fire retardant intumescent systems: Part I—Overall
543 thermal degradation," *Polym. Degrad. Stab.*, vol. 27, no. 3, pp. 285–296, 1990.
- 544 [19] C.-L. Deng, S.-L. Du, J. Zhao, Z.-Q. Shen, C. Deng, and Y.-Z. Wang, "An intumescent
545 flame retardant polypropylene system with simultaneously improved flame retardancy
546 and water resistance," *Polym. Degrad. Stab.*, vol. 108, pp. 97–107, 2014.

- 547 [20] S. Liang, N. Neisius, and S. Gaan, "Recent developments in flame retardant polymeric
548 coatings," *Prog. Org. Coatings*, vol. 76, pp. 1642–1665, 2013.
- 549 [21] Z. Liu, M. Dai, Y. Zhang, X. Gao, and Q. Zhang, "Preparation and performances of
550 novel waterborne intumescent fire retardant coatings," *Prog. Org. Coatings*, vol. 95,
551 pp. 100–106, 2016.
- 552 [22] S. Ullah, F. Ahmad, and P. S. M. M. Yusoff, "Effect of boric acid and melamine on the
553 intumescent fire-retardant coating composition for the fire protection of structural steel
554 substrates," *J. Appl. Polym. Sci.*, vol. 128, no. 5, pp. 2983–2993, 2013.
- 555 [23] A. Donmez Cavdar, F. Mengeloğlu, and K. Karakus, "Effect of boric acid and borax on
556 mechanical, fire and thermal properties of wood flour filled high density polyethylene
557 composites," *Measurement*, vol. 60, pp. 6–12, 2015.
- 558 [24] M. Jimenez, S. Duquesne, and S. Bourbigot, "Intumescent fire protective coating:
559 Toward a better understanding of their mechanism of action," *Thermochim. Acta*, vol.
560 449, no. 1, pp. 16–26, 2006.
- 561 [25] M. Jimenez, S. Duquesne, and S. Bourbigot, "High-Throughput Fire Testing for
562 Intumescent Coatings," *Ind. Eng. Chem. Res.*, vol. 45, no. 22, pp. 7475–7481, Oct.
563 2006.
- 564 [26] J. Lefebvre, V. Mamleev, M. Bras, and S. Bourbigot, "Kinetic analysis of pyrolysis of
565 cross-linked polymers," *Polym. Degrad. Stab. - POLYM Degrad STABIL*, vol. 88, pp.
566 85–91, Apr. 2005.
- 567 [27] S. Bourbigot, J. Gilman, and C. Wilkie, "Kinetic analysis of the thermal degradation of
568 polystyrene–montmorillonite nanocomposite," *Polym. Degrad. Stab.*, vol. 84, pp. 483–
569 492, Jun. 2004.
- 570 [28] S. Thumsorn, K. Yamada, Y. W. Leong, and H. Hamada, "Thermal decomposition
571 kinetic and flame retardancy of CaCO₃ filled recycled polyethylene
572 terephthalate/recycled polypropylene blend," *J. Appl. Polym. Sci.*, vol. 127, no. 2, pp.
573 1245–1256, 2013.
- 574 [29] Z. Wang, F. Jia, E. R. Galea, and J. Ewer, "Computational Fluid Dynamics Simulation
575 of a Post-Crash Aircraft Fire Test," *J. Aircr.*, vol. 50, no. 1, pp. 164–175, 2013.
- 576 [30] B. Song, X. Wang, and H. Zhang, "The Aircraft Composite Integral Fuel Tank Fire

- 577 Safety Performance Analysis and Shrinkage Ratio Simulation Calculation,” *Procedia*
578 *Eng.*, vol. 52, pp. 320–324, 2013.
- 579 [31] N. Grange, K. Chetehouna, N. Gascoin, and S. Senave, “Numerical investigation of the
580 heat transfer in an aeronautical composite material under fire stress,” *Fire Saf. J.*, vol.
581 80, pp. 56–63, 2016.
- 582 [32] I. Ali, N. K. Kim, and D. Bhattacharyya, “Effects of Graphene Nanoplatelets on
583 Mechanical and Fire Performance of Flax Polypropylene Composites with Intumescent
584 Flame Retardant,” *Molecules*, vol. 26, no. 13, 2021.
- 585 [33] M. Rashid, J. L. Hanus, K. Chetehouna, K. Khellil, Z. Aboura, and N. Gascoin,
586 “Investigation of the effect of tufts contribution on the in-plane mechanical properties
587 of flax fibre reinforced green biocomposite,” *Funct. Compos. Mater.*, vol. 2, no. 1, p.
588 11, 2021.
- 589 [34] J. Opfermann, “Kinetic Analysis Using Multivariate Non-linear Regression. I. Basic
590 concepts,” *J. Therm. Anal. Calorim.*, vol. 60, no. 2, pp. 641–658, 2000.
- 591 [35] M. E. Brown, D. Dollimore, and A. K. Galwey, “Theory of solid state reaction
592 kinetics,” *Compr. Chem. Kinet.*, vol. 22, pp. 41–113, 1980.
- 593 [36] S. Vyazovkin, “Kinetic concepts of thermally stimulated reactions in solids: A view
594 from a historical perspective,” *Int. Rev. Phys. Chem.*, vol. 19, no. 1, pp. 45–60, 2000.
- 595 [37] S. Vyazovkin *et al.*, “ICTAC Kinetics Committee recommendations for collecting
596 experimental thermal analysis data for kinetic computations,” *Thermochim. Acta*, vol.
597 590, pp. 1–23, 2014.
- 598 [38] M. E. Brown, Ed., “Thermogravimetry (TG),” in *Introduction to Thermal Analysis:
599 Techniques and Applications*, Dordrecht: Springer Netherlands, 2001, pp. 19–54.
- 600 [39] M. E. Brown, “The Prout-Tompkins rate equation in solid-state kinetics,” *Thermochim.*
601 *Acta*, vol. 300, no. 1, pp. 93–106, 1997.
- 602 [40] M. Rashid, K. Chetehouna, L. Lemée, C. Roudaut, and N. Gascoin, “Study of flame
603 retardancy effect on the thermal degradation of a new green biocomposite and
604 estimation of lower flammability limits of the gaseous emissions,” *J. Therm. Anal.*
605 *Calorim.*, 2022.

- 606 [41] S. Murat Unlu, U. Tayfun, B. Yildirim, and M. Dogan, "Effect of boron compounds on
607 fire protection properties of epoxy based intumescent coating," *Fire Mater.*, vol. 41,
608 no. 1, pp. 17–28, 2017.
- 609 [42] M. Jimenez, S. Duquesne, and S. Bourbigot, "Characterization of the performance of
610 an intumescent fire protective coating," *Surf. Coatings Technol.*, vol. 201, no. 3, pp.
611 979–987, 2006.
- 612 [43] A. K. Burnham and R. L. Braun, "Global Kinetic Analysis of Complex Materials,"
613 *Energy & Fuels*, vol. 13, no. 1, pp. 1–22, Jan. 1999.
- 614 [44] E. Moukhina, "Determination of kinetic mechanisms for reactions measured with
615 thermoanalytical instruments," *J. Therm. Anal. Calorim.*, vol. 109, no. 3, pp. 1203–
616 1214, 2012.
- 617 [45] P. Budrugaec, "The evaluation of the non-isothermal kinetic parameters of the thermal
618 and thermo-oxidative degradation of polymers and polymeric materials: its use and
619 abuse," *Polym. Degrad. Stab.*, vol. 71, no. 1, pp. 185–187, 2000.
- 620 [46] J. Opfermann, J. Blumm, and W.-D. Emmerich, "Simulation of the sintering behavior
621 of a ceramic green body using advanced thermokinetic analysis," *Thermochim. Acta*,
622 vol. 318, no. 1, pp. 213–220, 1998.
- 623 [47] A. Ramgobin, G. Fontaine, and S. Bourbigot, "A Case Study of Polyetheretherketone
624 (II): Playing with Oxygen Concentration and Modeling Thermal Decomposition of a
625 High-Performance Material.," *Polymers (Basel)*, vol. 12, no. 7, Jul. 2020.
- 626 [48] J. Opfermann and E. Kaisersberger, "An advantageous variant of the Ozawa-Flynn-
627 Wall analysis," *Thermochim. Acta*, vol. 203, pp. 167–175, 1992.
- 628 [49] P. Sharma, V. Choudhary, and A. K. Narula, "Effect of structure of aromatic imide–
629 amines on curing behavior and thermal stability of diglycidyl ether of bisphenol-A," *J.*
630 *Appl. Polym. Sci.*, vol. 107, no. 3, pp. 1946–1953, 2008.
- 631 [50] W. F. Mohamad, F. Ahmad, and S. Ullah, "Effect of Inorganic Fillers on Thermal
632 Performance and Char Morphology of Intumescent Fire Retardant Coating," *Asian J.*
633 *Sci. Res.*, vol. 6, pp. 263–271, 2013.
- 634 [51] Z. Li and B. Qu, "Flammability characterization and synergistic effects of expandable
635 graphite with magnesium hydroxide in halogen-free flame-retardant EVA blends,"

636 *Polym. Degrad. Stab.*, vol. 81, no. 3, pp. 401–408, 2003.

637